European Journal of Neuroscience, Vol. 26, pp. 3382–3394, 2007 doi:10.1111/j.1460-9568.2007.05954.x

Target regulation of V2R expression and functional maturation in vomeronasal sensory neurons *in vitro*

Kazuyo Muramoto,[1] Mitsuhiro Hashimoto[2] and Hideto Kaba[1,3]
[1]Department of Physiology, Kochi Medical School, Kohasu, Oko-cho, Nankoku, Kochi 783–8505, Japan
[2]Hashimoto Research Unit, Critical Period Mechanisms Research Group, Brain Science Institute, RIKEN, Wako, Saitama 351–0198, Japan
[3]Division of Adaptation Development, Department of Developmental Physiology, National Institute for Physiological Sciences, Okazaki, Aichi 444–8585, Japan

Keywords: accessory olfactory bulb, calcium imaging, coculture, mouse, rat

Abstract

Vomeronasal receptors from the *V1R* and *V2R* gene families mediate the detection of chemical stimuli such as pheromones via the vomeronasal organ (VNO). The differential expression of vomeronasal receptors might contribute in part to a variety of pheromonal effects, which are different sexually, developmentally and even individually. However, little is known about the mechanisms controlling vomeronasal receptor expression. Cultured vomeronasal sensory neurons (VSNs) bear phenotypic resemblance to the intact VNO but they remain immature. Because indices of VSN maturation are increased by coculture with the target cells for VSNs, accessory olfactory bulb (AOB) neurons, AOB neurons may regulate vomeronasal receptor expression and functional maturation in VSNs. To test this hypothesis, we examined the expression of V2R-type vomeronasal receptors (VR1 and VR4) and chemosensory responsiveness in VNOs cocultured with AOB neurons. Immunoblot and immunocytochemical analysis revealed that the coculture of VNOs with AOB neurons resulted in a greater expression of VR1 and VR4 after 10 days than VNOs cultured alone. Moreover, calcium imaging analysis showed that cocultured VNOs responded to urine components applied iontophoretically into their cavities with a time course similar to the V2R expression, in contrast to singly cultured VNOs that displayed no response. These results demonstrate that AOB neurons induce the expression of vomeronasal receptors in VSNs, allowing them to function.

Introduction

Many mammals detect pheromones by a unique structure, the vomeronasal organ (VNO), located in the base of the anterior nasal septum. The detection of pheromones affects endocrinological status and instinctive behaviours related to reproduction and social recognition in various kinds of animals (Wysocki, 1979; Halpern, 1987; Meredith, 1991). The repertoires of innate behaviours and neuroendocrine responses induced by pheromones differ remarkably between males, females and sexually immature animals (Halpern, 1987; Halpern & Martínez-Marcos, 2003). However, the precise cellular mechanisms regulating these differential functions are not well understood. The sexual dimorphism and age-related differences in pheromone perception may involve peripheral and/or central components of the vomeronasal system. One possible mechanism may rely on the differential expression of vomeronasal receptors in subpopulations of vomeronasal sensory neurons (VSNs).

The family of genes encoding vomeronasal receptors is composed of two distinct families, the *V1Rs* (Dulac & Axel, 1995) and *V2Rs* (Herrada & Dulac, 1997; Matsunami & Buck, 1997). *V1Rs* and *V2Rs* are expressed by distinct subpopulations of VSNs and, within each subpopulation, the expression of each receptor gene is confined to small and nonoverlapping subpopulations of the VSNs (Dulac, 2000; Mombaerts, 2004). Such an expression pattern suggests a model of vomeronasal signalling according to which the binding of pheromones to specific receptors leads to the activation of distinct subpopulations of VSNs, thus providing a possible mechanism for sensory discrimination among pheromonal signals. Interestingly, the distributions of expression of one V2R vary between males and females in rats, suggesting the existence of discrete and sexually dimorphic patterns of receptor expression (Herrada & Dulac, 1997). These differences may contribute to the sexually dimorphic effects of some pheromones.

Previously, we independently developed two primary culture systems for the VNO (Osada *et al*., 1999) and the accessory olfactory bulb (AOB; Muramoto *et al*., 2003). We recently reported that indices of VSN maturation in the culture were increased by coculture with dissociated AOB neurons (Moriya-Ito *et al*., 2005). Coculture of VSNs with AOB neurons results in the expression of olfactory marker protein (OMP) and the protrusion of microvilli (Moriya-Ito *et al*., 2005). These changes suggest that the expression of some vomeronasal receptor genes in the VNO is also induced by the interaction with cocultured AOB neurons. However, it has not been made clear whether or not the expression of vomeronasal receptors is regulated by AOB neurons; if so, how is the receptor expression related to the functional maturation of VSNs? In the present study, to characterize a regulatory mechanism for the maturation of pheromonal recognition we examined changes in the expression of two representatives (VR1 and VR4; Matsunami & Buck, 1997) from the V2R family of vomeronasal receptors and changes in responsiveness to urine

Correspondence: Dr Kazuyo Muramoto, as above.
E-mail: tkazuyo@kochi-u.ac.jp

Received 10 September 2007, revised 13 October 2007, accepted 18 October 2007

components in the cultured VNO in the presence or absence of the cultured AOB neurons. We show here that VSNs cocultured with AOB neurons display an enhanced expression of V2R-type vomeronasal receptors in parallel with the acquisition of functional responsiveness to urine components.

Materials and methods

Cell culture

All animal experiments were approved by the Kochi Medical School Animal Care and Use Committee and carried out in accordance with the Guidelines for Animal Experiments of Kochi Medical School and the Japanese Animal Protection and Management Law. All efforts were made to minimize the number of animals used.

Primary cultures of dissociated AOB cells were prepared from Wistar rats at embryonic day (E)19 following a previously reported procedure (Muramoto *et al*., 2003, 2004, 2006; Kato-Negishi *et al.,* 2003). In brief, the pregnant rats were killed by decapitation after inhaling excess diethyl ether, and then their uteri were dissected out. After removing the brains from the decapitated E19 embryonic rats, the AOBs were dissected out and pooled, and then enzymatically dissociated with papain (Worthington Biochemical Corp., Freehold, NJ, USA). The AOB cells were plated at a density of 1.6×10^5 cells/cm^2 on 35-mm-diameter glass-bottomed dishes (10 mm diameter glass hole; Matsunami Glass Ind., Ltd, Osaka, Japan) or 35-mm-diameter plastic dishes. After maintaining AOB neurons for 7 days *in vitro* (DIV), the coculture was started by transferring some VNOs onto them.

Organ cultures of VNOs were prepared from Wistar rats on E15 with a modification of the previously described method (Osada *et al*., 1999; Moriya-Ito *et al*., 2005). The embryonic rats were removed from uteri, after the pregnant rats were killed in the same way as for the AOB culture procedure. The VNOs were excised from the heads of decapitated embryonic rats, and pooled. When the VNOs are enzymatically digested and partially dissociated, after 7–14 DIV plated VSNs form a spherical structure with a central cavity (Osada *et al*., 1999), whose morphological characteristics resemble those of the intact vomeronasal epithelium. We referred to this spherical structure as the vomeronasal pocket (VNP). However, the VNP would contain limited subpopulations of VSNs. To evaluate the receptor expression and the responsiveness to urine of the VNO it would be ideal to maintain a tissue organization that closely resembles that observed *in situ*, so we used the whole VNO without enzyme digestion for the culture instead of the VNP. The VNOs were plated onto 35-mm-diameter plastic dishes covered with a feeder cell layer (Osada *et al*., 1999), which originated from a VNO culture maintained in a serum-containing medium. These feeder cells appeared to be VNO-derived fibroblasts or chondroblasts.

After VNOs were maintained for 10 DIV, they were transferred using a micropipette onto dishes containing the AOB culture; this time was designated 0 days in coculture (DICC; Muramoto *et al*. 2003, 2006; Moriya-Ito *et al*., 2005). For the control experiment, VNOs in the same culture period were transferred onto dishes containing other VNO-derived feeder cells (VNO-alone culture).

Antibodies and immunoblotting

Synthetic peptides of the COOH-termini of VR1 (NH_2-CPDSNF-IKNHKGKLLY-COOH) and VR4 (NH_2-CPERNSTQKIREKSYF-COOH) were conjugated to keyhole limpet haemocyanin using m-maleimidobenzoyl-N-hydroxysuccinimide ester as crosslinker. Each immunogen was inoculated into rabbits. Specific antibodies against VR1 and VR4 were affinity-purified from the immunized rabbit plasma using affinity columns (Sulfolink column; Pierce) conjugated to each peptide. Probing with anti-β-actin antibody (Chemicon, Temecula, CA, USA) served as an internal control for protein loading and expression. The level of VR1 and VR4 expression was corrected so that β-actin is expressed at a level similar to that in the samples examined.

After culturing for designated periods with or without AOB neurons, 75–120 cultured VNOs were collected from each experimental condition and in a solution containing: NP-40, 1%; sucrose, 0.25 M; and Tris-HCl, pH 7.5, 25 mM; supplemented with 1% protease inhibitor cocktail (Set III; Calbiochem, San Diego, CA, USA). After brief centrifugation, the supernatant was collected and an equal volume of 2× concentrated SDS sample buffer (Tris-HCl, pH 6.8, 125 mM; 2-mercaptoethanol, 10%; SDS, 4%; glycerol, 10%; and bromophenol blue, 0.008%; all purchased from Sigma-Aldrich) was added. Such samples were subjected to 7.5% SDS-polyacrylamide gel electrophoresis and transferred onto a PVDF membrane (Millipore, Bedford, MA, USA). After blocking with 1% skimmed milk, the blotted membrane was incubated overnight with one of three antibodies, i.e. anti-VR1, anti-VR4 or anti-β-actin antibody. After incubating with horseradish peroxidase-conjugated anti-rabbit Ig (for anti-VR1 and VR4) or anti-mouse Ig (for anti-β-actin) antibodies (both GE Healthcare Bio-Science Co., Piscataway, NJ, USA), the immunoreactions were visualized using the ECL plus Western blotting detection system (GE Healthcare Bio-Science). Images of immunoreactive bands were captured using Light Capture (Model AE-6961FC; Atto, Tokyo, Japan) and were densitometrically measured using public domain Image-J software (developed at the US National Institutes of Health).

Absorption tests with antibodies and synthetic antigen peptides were performed with serially diluted 10-mg/mL solutions of synthetic peptides in phosphate-buffered saline (PBS; pH = 7.2). Equal volumes of two-fold serially diluted peptide solutions and either control or antibodies were incubated for 1 h at room temperature and then used in the immunoblotting analyses as described above.

Immunocytochemistry

The tissues including the VNOs were dissected out from deeply anaesthetized female mice (C57BL6, postnatal day 21). The dissected tissues, cocultured VNOs at 21 DICC and the singly cultured VNOs at the corresponding DIV (31 DIV) were fixed with 4% paraformaldehyde in PBS for 1 h at room temperature. These fixed materials were then stored in 20% sucrose in PBS at 4 °C overnight. Cryosections (20 μm thick) were cut using a freezing microtome (Cryocut 1500; Leica) mounted onto Matsunami Adhesive Silan-coated glass slides (Matsunami, Japan). Mounted sections were rinsed with PBS and then incubated with blocking buffer (0.1% Triton X-100 and 1% skimmed milk in PBS) for 1 h at room temperature. Sections were then incubated overnight with primary antibodies in appropriate dilutions at 4 °C. Primary antibodies were used as follows: the rabbit anti-VR1 and VR4 antibodies were diluted 1 : 50 and the mouse monoclonal anti-β-tubulin class III (tubulin-βIII) antibody (R & D Biosystems, Inc., Minneapolis, MN, USA) was diluted 1 : 250 with blocking buffer. After washing three times in PBS for at least 10 min each, sections were incubated with secondary antibodies diluted with blocking buffer for 2 h at room temperature to visualize fluorescence. Immunoreactivities were visualized using Cy3-labelled anti-mouse IgG antibody (for tubulin-βIII; Jackson Immuno Research Laboratories, Inc., West Grove, PA, USA), and FITC-labelled anti-rabbit Ig

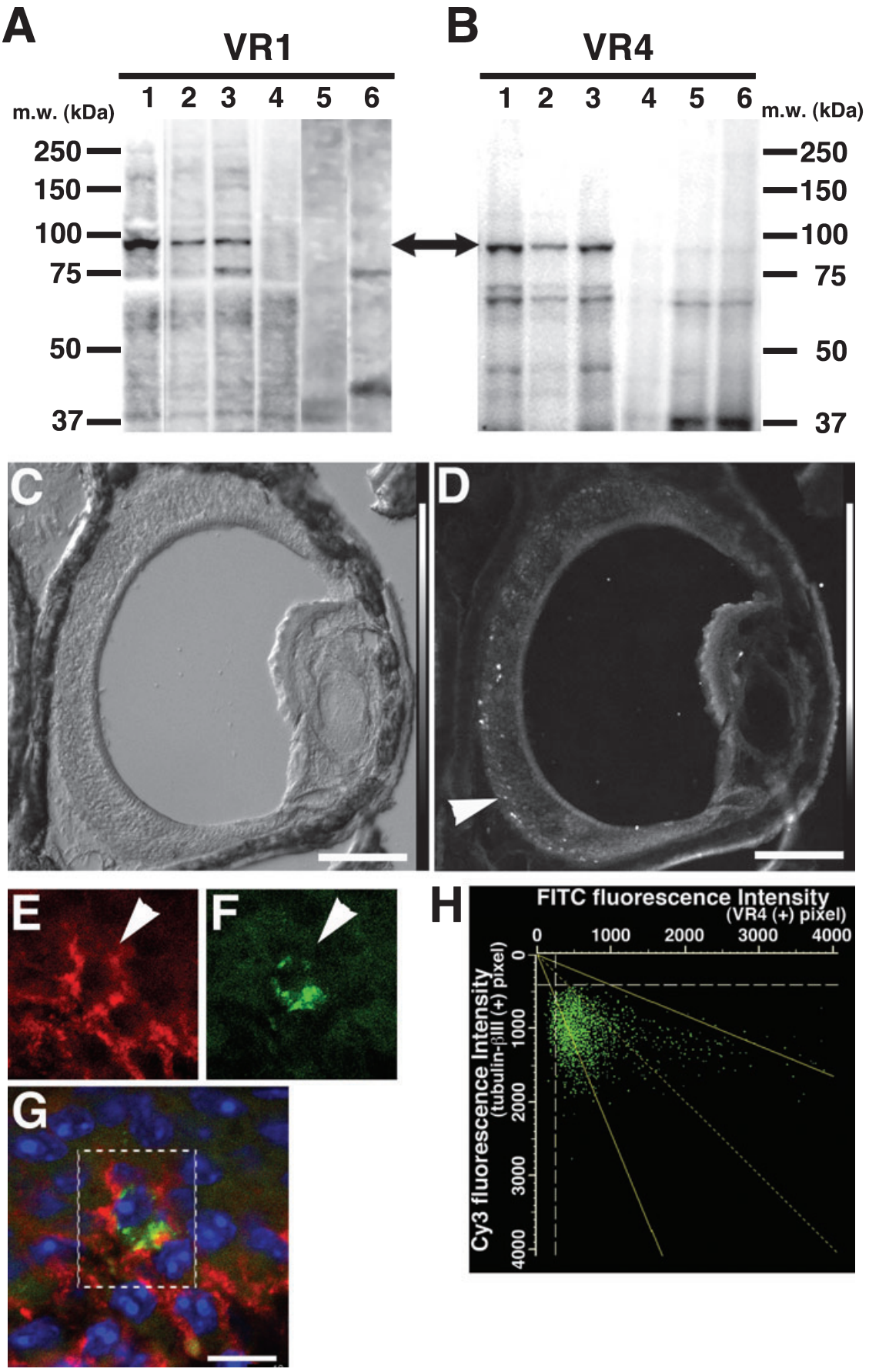

antibody (for VR1 and VR4; ICN Pharmaceuticals, Aurora, OH, USA). Cell nuclei were labelled with 1 μg/mL DAPI (4,6-diamidine-2-phenyl-indol-dihydrochlorid; Kirkegaard & Perry Laboratories, Inc., Washington, DC, USA) in PBS. Sections were washed again in PBS and then mounted with water-based mountant (FluorGuard; Bio-Rad). Images were captured using an Axiovert 100M inverted laser confocal microscope (LSM) system (LSM 510 Pascal; Carl Zeiss) and Eclipse TE2000 inverted LSM system (C1si-PFS; Nikon Instruments, Inc., Kawasaki, Japan).

The extent of colocalization of VR4 and tubulin-βIII was determined using the Nikon EZ-C1 software, in which the Manders' colocalization coefficient (M_x) was calculated by the following equation:

$$M_x = \frac{\sum_i x_{i,\mathrm{coloc}}}{\sum_i x_i}$$

where $x_{i,\mathrm{coloc}}$ is the value of pixel i of the overlapped FITC (VR4) and Cy3 (tubulin-βIII) components, and x_i is the value of pixel i of the FITC component (Manders *et al*., 1983).

Pearson's correlation coefficient (r) was calculated to describe the correlation between the intensity distributions of FITC (VR4) and Cy3 (tubulin-βIII) components with following equation:

$$r = \frac{\sum_i (x_i - x_{\mathrm{aver}}) \cdot (y_i - y_{\mathrm{aver}})}{\sqrt{\left[\sum_i (x_i - x_{\mathrm{aver}})^2 \cdot (y_i - y_{\mathrm{aver}})^2\right]}}$$

where x_i and y_i are the values of pixel i of the FITC and Cy3 components, respectively. The r-value is calculated between −1 and +1, which indicate negative and positive correlations, respectively, between FITC and Cy3 signals (Manders *et al*., 1983).

Iontophoretic application of diluted urine into the cavity of the cultured VNO

Urine was collected from an adult male mouse (BALB/c) and an adult male rat (Wistar). Both kinds of urine were diluted at a ratio of 1 : 9 with a basal salt solution (BSS; pH = 7.4; Muramoto *et al*., 2006) supplemented with 1.5 μM bromophenol blue to mark successful ejection. The cultured VNOs were loaded with the fluorescence calcium indicator fluo-4/AM (Molecular Probes, Eugene, OR, USA), and were observed using an imaging system (Aquacosmos; Hamamatsu Photonics, Hamamatsu, Japan). The fluo-4-loaded VNO was impaled with a three-barrelled glass microelectrode. Each barrel of the microelectrode was filled with one of the following solutions: diluted urine; BSS; artificial urine consisting of (in mM): NaCl, 120; KCl, 40; NH_4OH, 20; $CaCl_2$, 4; $MgCl_2$, 2.5; NaH_2PO_4, 15; $NaHSO_4$, 20; and urea, 333; adjusted to pH 7.4 with NaOH (Leypold *et al*., 2002). Artificial urine was also diluted 1 : 9 with BSS. Charged compounds in urine were iontophoretically ejected into the central cavity of VNO using a microiontophoresis apparatus (Model SEZ-3104; Nihon-Koden, Tokyo, Japan) while fluorescent images were recorded.

Calcium imaging

The fluo-4/AM stock solution (1 mM in dimethyl sulfoxide) was diluted to a final concentration of 2 μM with BSS. After fluo-4 was loaded into the cocultured VNP and AOB neurons, it was observed using an imaging system (Aquacosmos), which was composed of an inverted fluorescence microscope (Axiovert S100; Zeiss) equipped with a highly sensitive cooled CCD camera (Orca ER; C4742-95–12ER; Hamamatsu Photonics) and an image analysing system (Muramoto *et al*., 2006). Fluorescent images were recorded at a rate of 1–4 images per second on a hard disk for 3–6 min and analysed using *ad hoc* hardware and software. Images were captured using the same voltage gain, exposure time and other settings. All recordings were performed at room temperature (20–24 °C).

Image processing and data analysis

To quantitatively evaluate the responses of the VNO to charged compounds in the urine under the various conditions, we measured the ratio of the areas showing urine-elicited responses to the whole areas of each VNO on fluorescence images (relative response area). To determine such areas we used the subtraction image, which was made by subtracting an image made before iontophoretic ejection from an image made just after iontophoretic ejection. The 15–30 sequential images from both before and during current ejection were captured, and then were independently averaged to make a subtraction image. An averaged image made from images before current ejection shows the resting state of the cultured VNO, and that during current ejection represents the excited state of the cultured VNO. The averaged image in the resting state was subtracted from that in the excited state. We defined the remaining area showing fluorescence signals in these subtraction images as the relative response area.

Subtraction images (512 × 512 pixels) were made as 8-bit (256 gradation) grey-scale images. When the relative response area was quantitatively measured, firstly the subtraction images were converted into binary images. To convert into binary images, values < 75 of the 256 gradations in the original subtraction image were cut off as noise. Averaging and subtraction of images were performed using the Aquacosmos analysing software. The Image-J software was used for making binary images and measurement for the relative response area.

FIG. 1. (A) Immunoblots of homogenates from different samples using anti-VR1 antibodies. The anti-VR1 antibody reacts with homogenates of intact VNO from adult BALB/c mice (lane 1), adult Wistar rats (lane 2) and rat VNO cocultured with AOB neurons (lane 3). In the coculture, VNOs were cultured alone for 10 days, transferred onto the cultured AOB neurons and maintained for an additional 15 days. An anti-VR1 antibody is absorbed with the synthetic antigen peptide and subsequently tested in the Western blot assay for homogenates from intact mouse (lane 4) and rat (lane 5) VNO, and cocultured rat VNO (lane 6). (B) Immunoblots of homogenates using anti-VR4 antibodies. All lanes correspond to those in A. The bidirectional arrow between A and B indicates bands immunoreactive to the V2R family of vomeronasal receptors. (C) The differential interference contrast (DIC) image of a VNO cryosection prepared from a female mouse (postnatal day 21). (D) The fluorescence image of the section in C stained with anti-VR4 antibody. Relatively large numbers of VR4-immunopositive puncta were observed. (E–G) Magnified images of the region, indicated by arrowhead in D, costained for (E) tubulin-βIII and (F) VR4 (G is the merged image where cell nuclei were counterstained blue with DAPI) showing the colocalization of tubulin-βIII and VR4 in the same cell. (H) Scatter diagram showing the distributions of fluorescence intensity of each pixel for VR4 (FITC, x-coordinate) and tubulin-βIII (Cy3, y-coordinate) images. Each pixel of the diagram shows where pixels from the two source images coincide. Data are obtained from the rectangular region in G. Scale bars, 100 μm (C and D), 10 μm (G).

Statistical analysis

The statistical analysis was performed with StatView® (SAS Institute, Inc.) software.

Results

Expression of VR1 and VR4 in cultured rat VNOs

To examine changes in the expression of the V2R family of vomeronasal receptors, we used specific antibodies against two representatives (VR1 and VR4) of the V2R family. Because both of the antibodies were produced using synthetic peptides based on mouse amino acid sequences for VR1 and VR4 as antigens, we first checked their cross-reactivity to each of the rat homologues using immunoblot analysis (Fig. 1A and B). Immunoblotting using an anti-VR1 antibody was able to detect an ~90 kDa or higher band in the lane of the whole homogenate prepared from intact rat VNOs (Fig. 1A, VR1-lane 2) as well as intact mouse VNOs (Fig. 1A, VR1-lane 1). Such molecular weight bands were similarly observed using an anti-VR4 antibody on the mouse (Fig. 1B, VR4-lane 1) and the rat (Fig. 1A, VR4-lane 2) intact VNO homogenates. These bands corresponded to the estimated molecular weight for most of the V2R family receptor proteins.

Similar bands were observed in lanes of homogenates prepared from the rat VNO cocultured with the AOB, in which VNOs at 10 DIV were transferred onto the cultured AOB cells and maintained for an additional 15 DICC (Fig. 1A and B, VR1-lane 3, VR4-lane 3).

The ~90-kDa bands in three lanes of the different homogenates, each of which was immunoreactive for anti-VR1 or -VR4 antibodies, completely disappeared after preincubating the antibody solutions with antigen peptides (Fig. 1A and B, lane 4–6), suggesting that these bands included the antigenic epitopes in the V2R family of vomeronasal receptors.

To further characterize these V2R antibodies used in the present study, we stained cryosections of intact female mouse VNOs (postnatal day 21; Fig. 1C) using an immunofluorescence method (Fig. 1D). More cells than expected could be stained with the anti-VR4 antibody in VNO sections (Fig. 1D), while VR1-immunostained cells were rarely distributed in VNO sections (data not shown). Most of these V2R-immunopositive cells could be superimposed on tubulin-βIII-immunopositive cells (Fig. 1E–G). These results suggest that the anti-VR4 antibody cross-reacts with a proportion of vomeronasal receptor types and the anti-VR1 antibody specifically reacts with fewer receptor types. The colocalization of VR4 and tubulin-βIII was analysed with a scatter diagram (Fig. 1H) of common pixels in the two superimposed images of Fig. 1G. Manders' colocalization coefficient (M_x) was 78%, indicating that VR4 immunoreactivities were colocalized with tubulin-βIII immunoreactivities (Fig. 1H). The localizations of the two proteins were weakly correlated with each other (Pearson's correlation coefficient $r = 0.32$). This weak correlation is probably because it is unlikely that the subcellular distributions of the two proteins are completely coincident, viz. $r = 1$. The colocalization analyses indicate that the VR4-immunopositive cells are identical to tubulin-βIII-positive VSNs.

Increases in VR1 and VR4 expression in VNOs cocultured with AOB neurons

Next, we examined quantitative changes in the expression of VR1 and VR4 over time in culture (Fig. 2). For the coculture with AOB cells, cultured VNOs were maintained alone for 10 DIV from the beginning

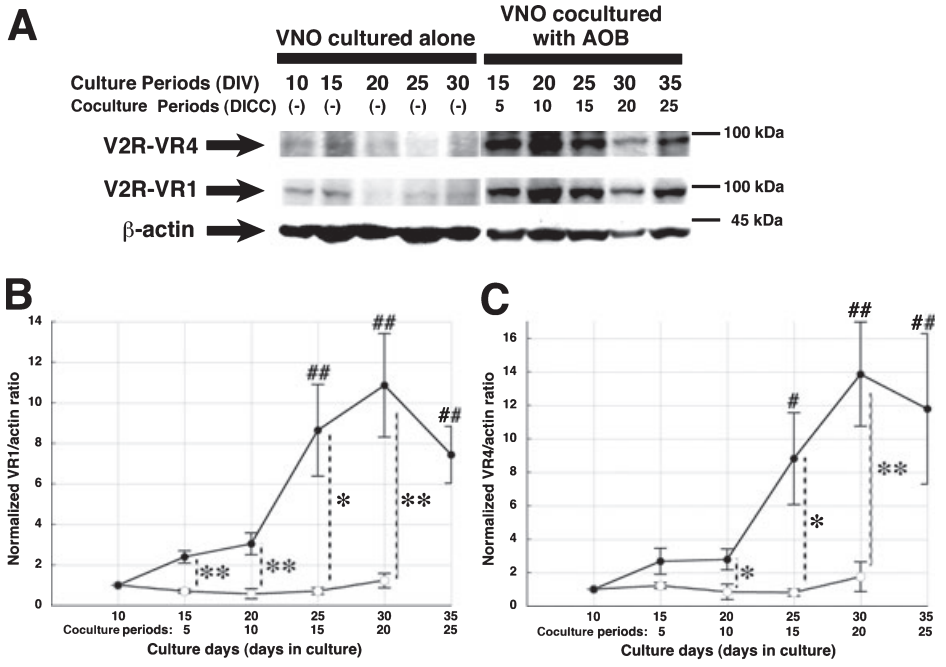

FIG. 2. Coculture of VNO with AOB cells resulted in increased expression of V2R vomeronasal receptors. (A) Representative immunoblots of VNO proteins prepared from the VNO-alone culture and VNO–AOB coculture, and probed with anti-VR4, VR1 and β-actin antibodies. The optical density of immunoreactive bands was measured by densitometry and values relative to the β-actin levels are calculated. Each value at 10 DIV was taken as normalized 1.0, as shown in (B) and (C). (B) Change in VR1 expression over the culture periods. (C) Change in VR4 expression over the culture periods. Data are represented as means ± SEM (the mean expression ratio of each V2R to β-actin; $n = 4$). Open and closed circles in B and C indicate V2R expression in the singly cultured VNO and cocultured VNO, respectively. Two-way ANOVA for repeated measures was used, followed by a Tukey–Kramer multiple comparison test and Dunnett's test: $^{*}P < 0.05$, $^{**}P < 0.01$ vs. VNO-alone culture at the corresponding time point; $^{\#}P < 0.05$, $^{\#\#}P < 0.01$ vs. coculture at 0 DICC.

of the culture. They were then excised from the feeder layer and transferred onto the cultured AOB cells, i.e. 10 DIV means 0 DICC. Thereafter, cocultured VNOs were harvested at a given DICC and examined.

The immunoreactivities against VR1 and VR4 bands in the VNO cocultured with the AOB cells were much stronger than those in the VNO cultured alone (Fig. 2A). Semiquantitative analysis using the optical density of the immunoreactive bands revealed that the expression of both V2Rs in the cultured VNOs was significantly enhanced by coculturing with AOB cells (the data are given as the 'expression ratios' of each V2R to β-actin, appearing as a 42-kDa band; Fig. 2B and C). An ANOVA for repeated measures detected a significant difference in the mean expression ratios of both V2Rs between the coculture and the VNO-alone culture (VR1, $F_{1,4} = 19.67$, $P < 0.01$; VR4, $F_{1,4} = 14.47$, $P < 0.01$). A subsequent analysis of the means using the Tukey–Kramer multiple comparison test indicated that the mean expression ratios of VR1 in the VNO coculturing with the AOB cells after 5 DICC differed significantly from those in the VNO cultured alone at the corresponding DIV ($P < 0.01$ at 5, 10 and 20 DICC; $P < 0.05$ at 15 DICC). Similarly, the mean expression ratios of VR4 in the VNO coculturing with the AOB cells after 10 DICC differed significantly from those in the VNO cultured alone at the corresponding DIV ($P < 0.01$ at 20 DICC; $P < 0.05$ at 10 and 15 DICC). Furthermore, the mean expression ratios of both V2Rs significantly increased over 0 DICC values after 15 DICC and reached a plateau at 20 DICC (VR1, $P < 0.01$ at 15, 20 and 25 DICC; VR4, $P < 0.05$ at 15 DICC, $P < 0.01$ at 20 and 25 DICC; Dunnett's test; Fig. 2B and C). In contrast, the mean expression ratios of both V2Rs in the VNO-alone culture were not significantly changed at any time during the culture period (Fig. 2B and C).

Localization of vomeronasal receptors in the cultured VNO after their expression was induced

To confirm the expression and the localization of V2Rs at the cultured tissue level, we immunocytochemically stained cryosections of VNOs cocultured with AOB cells using an anti-VR4 rabbit antibody and an anti-tubulin-βIII mouse monoclonal antibody at 21 DICC. As a control, VNOs cultured alone were also stained at the same culture period (31 DIV). As shown in Fig. 3, more tubulin-βIII-immunopositive cells were observed throughout the cocultured VNO cryosection (Fig. 3B) than those in the VNO cultured alone (Fig. 3L). Such immunoreactivity indicated that these cells were neurons, i.e. VSNs. A small number of these cells also showed immunoreactivity to VR4, which was strongly observed around somata (Fig. 3A–G, arrowheads). It was obvious that VR4-immunopositive VSNs increased in number by interacting with AOB cells. The colocalization of VR4 and tubulin-βIII was estimated as 81% (M_x), and their localizations were correlated with each other ($r = 0.40$; Fig. 3H), indicating that the VR4-immunoreactive cells were VSNs. These values were closely equivalent to ones for the VNO tissue sections (Fig. 1H). Moreover, another view of the cocultured VNO stained with anti-VR4 antibody showed that a particularly strong VR4-immunopositive region was observed on the border of the cell layer facing the central cavity (Fig. 3I). Such a region might correspond to the layer from which microvilli protrude. In some cocultured VSNs, the VR4 immunoreactivities could be observed not only in soma but also along the dendritic processes extending toward the central cavity of the cultured VNO (Fig. 3J). Such an immunostaining pattern was not observed in the VNO cultured alone in the same culture period (Fig. 3K–M).

Application of charged compounds in mouse urine elicited responses in cultured VNO in the presence of cultured AOB neurons

To extend the validity of the finding that the expression of V2R family pheromone receptors is enhanced by interacting with the AOB neurons, we further examined functionally whether the responses of cultured VSNs to pheromonal compounds through their receptors differed between the presence and absence of the cultured AOB neurons. Even after starting the coculture with AOB neurons, the spherical structure of the VNO was maintained throughout the experimental period. Because receptive regions of VSNs, including microvilli, protrude into the central cavity of the cultured VNO (Moriya-Ito *et al*., 2005), stimulants should be injected into the cavity. Therefore, we applied pheromonal stimulants iontophoretically into the central cavity of the VNO through a three-barrelled glass microelectrode and then observed the responses of the VSNs with a calcium imaging technique using a fluorescent calcium indicator, fluo-4 (Fig. 4A).

Firstly, we checked whether urine from rats could evoke responses in cocultured rat VNOs. Urine collected from adult male rats was used as a stimulant. When charged compounds in the male rat urine were iontophoretically applied with a current of −2 μA into the cavity of cocultured VNO at 14 DICC (Fig. 4A), increases in the fluorescence intensity were observed (Fig. 4B, C and E). Rat urine diluted 1 : 100 with BSS evoked VNO responses in relatively small regions (Fig. 4, B-1 and -2). Then, rat urine diluted 1 : 10 with BSS evoked responses in more extended regions and their amplitudes were larger than those for urine diluted 1 : 100 (Fig. 4B and C). These increases in fluorescence intensity were not observed when artificial urine was iontophoretically applied into the VNO cocultured with AOB cells for 14 DICC with a negative current (Fig. 4, D-1 and D-2). Again, when charged compounds in the urine were iontophoretically applied into the same VNO with a negative current, the increases in the fluorescence intensity were reproduced (Fig. 4, E-1 and E-2). When rat urine was iontophoretically applied into the cocultured VNO it elicited VNO responses.

Mouse urine has been shown to contain volatile and nonvolatile pheromones, some of which have been well characterized (Brennan & Zufall, 2006). For example, recent evidence has demonstrated that major histocompatibility complex (MHC)-related peptides and major urinary proteins (MUP) function as chemosignals of individuality in the context of pregnancy block (Leinders-Zufall *et al*., 2004) and territorial behaviour (Humphries *et al*., 1999; Hurst *et al*., 2001; Wyatt, 2003), respectively. One of our main aims in a series of studies is to elucidate how they are encoded and processed in the culture system. With this view in mind, we used mouse urine as a stimulant. Urine collected from adult male mice was diluted with BSS.

The nature of the urine-elicited responses of the cocultured VNO was further examined (C. 5A and B). When charged compounds in the male mouse urine were iontophoretically applied into the cavity of cultured VNO at 14 DICC with a negative current of −1.5 μA, phasic increases in the fluorescence intensity were observed in limited regions of the VNO (Fig. 5, C-1 and -2). The subtraction image, which was made by subtracting an image before ejection from an image after ejection, clearly showed a more limited region in the VNO responding to charged compounds in the male mouse urine (Fig. 5, C-1). However, when a reversed current of +1.5 μA was applied through the same barrel, the cultured VNO did not show any response (Fig. 5, D-1 and D-2). Further, when artificial urine, which mimicked the electrolytic composition of the mouse natural urine, was used for iontophoretic ejection, the same VNO did not show any fluorescence

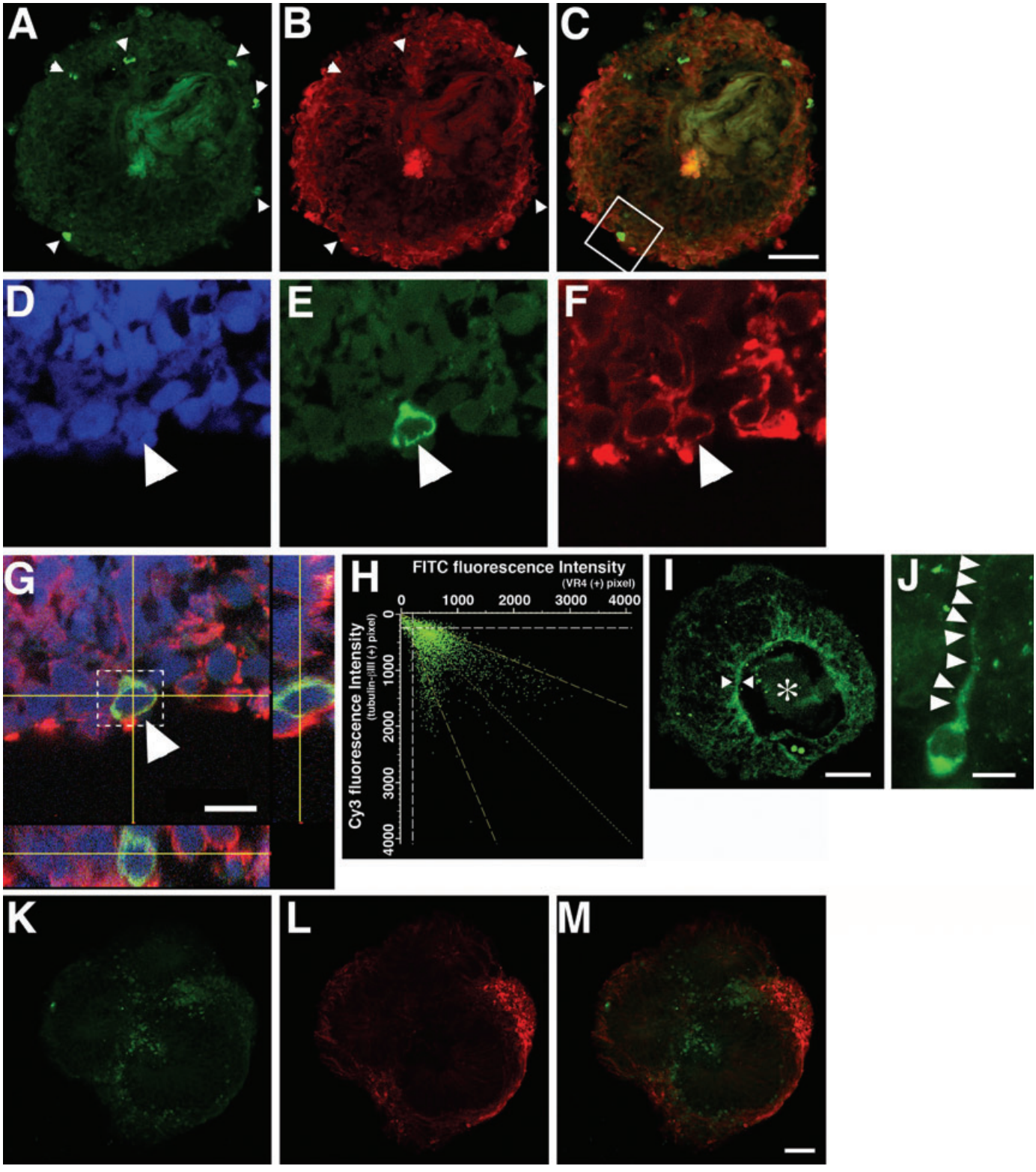

FIG. 3. Localization of VR4 in the cultured VNO. The cultured VNO was immunocytochemically stained using anti-VR4 and anti-tubulin-βIII antibodies at 21 DICC or at the corresponding time in the VNO-alone culture. (A–C) Co-staining for (A) VR4 and (B) tubulin-βIII (C is the merged image) in the cocultured VNO. (D–G) Magnified images of the rectangular region in C, costained for (D) cell nuclei, (E) VR4 and (F) tubulin-βIII (G is the merged image). (G) The compressed confocal *Z*-series is shown with orthogonal views taken at the levels indicated by the yellow lines. These images demonstrate the colocalization of VR4 and tubulin-βIII in the same cells (indicated by arrowheads in A–G). (H) Scatter diagram showing the distributions of fluorescence intensity of each pixel for VR4 (FITC, *x*-coordinate) and tubulin-βIII (Cy3, *y*-coordinate) images. Data were obtained from the rectangular region in G. (I) Another view of cocultured VNO with AOB neurons. The VR4 immunoreactivities are observed on the border of a cell layer (indicated by two arrowheads) facing the central cavity (asterisk). (J) A representative image of a VR4-immunopositive VSN. Arrowheads indicate dendritic process. (K–M) Co-staining for (K) VR4 and (L) tubulin-βIII (M is the merged image) in the VNO-alone culture showing that the localization of two proteins is not obvious. Scale bars, 50 μm (C, I and M), 10 μm (G and J).

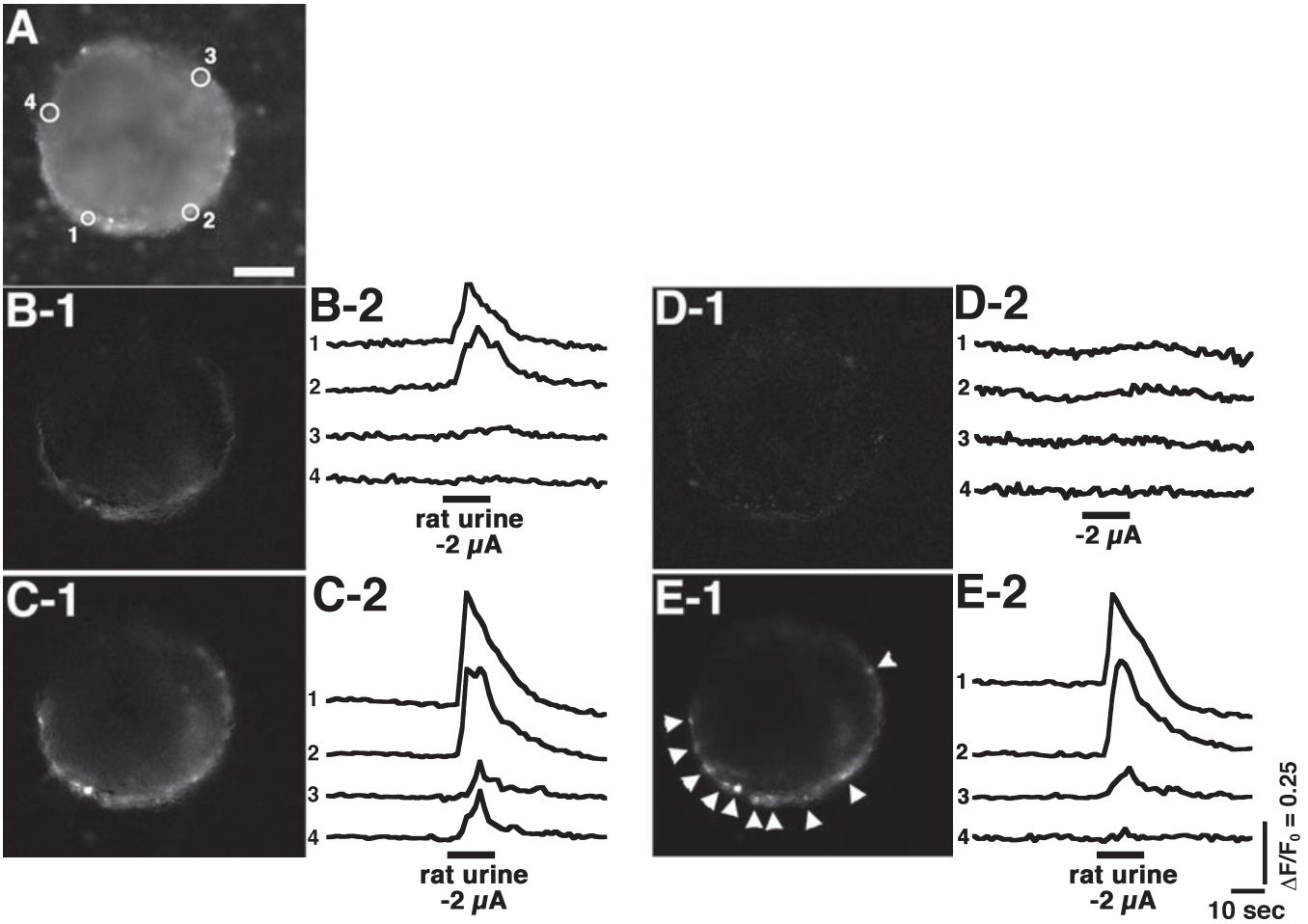

FIG. 4. The VNO cocultured with AOB cells also responded to rat urine. Currents were ejected through a three-barrelled glass microelectrode into the cavity of the VNO at 14 DICC. (A) Fluo-4 fluorescence image of cultured VNO showing regions of interest (ROIs), from which changes in fluorescence intensity were recorded. The numbers (1–4) of ROIs correspond to the numbered traces in B-2, C-2, D-2 and E-2. (B-1-E-1) The subtraction images were calculated as $F - F_0$ (F, the average of 20 fluorescence images during current ejection; F_0, the average of 30 fluorescence images just before current ejection). Stimulation protocols were the following: (B-1) rat urine diluted 1 : 100 with the BSS, with a current of −2.0 μA; (C-1) rat urine diluted 1 : 10 with the BSS, with a current of −2.0 μA; (D-1) artificial urine diluted 1 : 10 with BSS, with a current of −2.0 μA; (E-1) rat urine diluted 1 : 10 with the BSS, with a current of −2.0 μA, again. (B-2–E-2) Time course of changes in fluorescence intensity recorded from the four ROIs shown in A. The application of rat urine with a current of −2.0 μA (B-2, C-2 and E-2) evoked increases in fluorescence intensity, whereas the application of artificial urine had no effects on fluorescence intensity (D-2). Strong fluorescence changes were observed as particle-like round structures along the peripherally surrounding region of the VNO (indicated by arrowheads in E-1). These structures are possibly single VSNs.

changes when applying either negative (−1.5 μA; Fig. 5, E-1 and E-2) or positive (+ 1.5 μA; Fig. 5, F-1 and F-2) currents. Finally, when charged compounds in the urine were iontophoretically applied again into the same VNO with a negative current, the increases in fluorescence intensity were reproduced (Fig. 5, G-1 and G-2).

These urine-elicited responses in the VNO could be observed only under coculture with AOB cells. The VNOs, cultured for 10 DIV, were transferred on a feeder cell layer which was derived from a subculture of the VNO culture. The transferred VNOs were maintained for an additional 14 days and then tested for their responses to urine. In the absence of AOB cells, the VNOs were unable to respond to the iontophoretic application with negative current of charged compounds in the male mouse urine (Fig. 6A–C). Moreover, we tested the responsiveness of VNOs cocultured with AOB neurons to urine at an early time point in the coculture (7 DICC; Fig. 6D–F). The VNOs at 7 DICC showed no response to urine. This suggests that VNOs at 7 DICC were still immature.

To quantitatively evaluate the responses of the VNO to charged compounds in the urine under various conditions, we measured the ratio of the areas showing urine-elicited responses to the whole areas of each VNO on fluorescence images (relative response area; Fig. 7). To determine the area showing urine-elicited responses we used a subtraction image, which was made by subtracting an image made before iontophoretic ejection from an image made just after iontophoretic ejection. Charged compounds in the mouse (at 7, 14 and 21 DICC) and rat (only at 14 DICC) urine were iontophoretically ejected into the cultured VNO with a negative current from −1.5 to −2.0 μA (urine group). Artificial urine was used as a control (control group). The mean relative response area in the cocultured VNO at 7 DICC was not significantly different between the urine group (3.3 ± 1.0%, $n = 7$) and the control group (2.3 ± 0.76%, $n = 7$; Fig. 7). However, the mean relative response areas in the cocultured VNO at 14 and 21 DICC were significantly larger in the urine groups (mouse urine: 20.1 ± 4.6%, $n = 7$ at 14 DICC; 15.5 ± 1.4%, $n = 7$ at

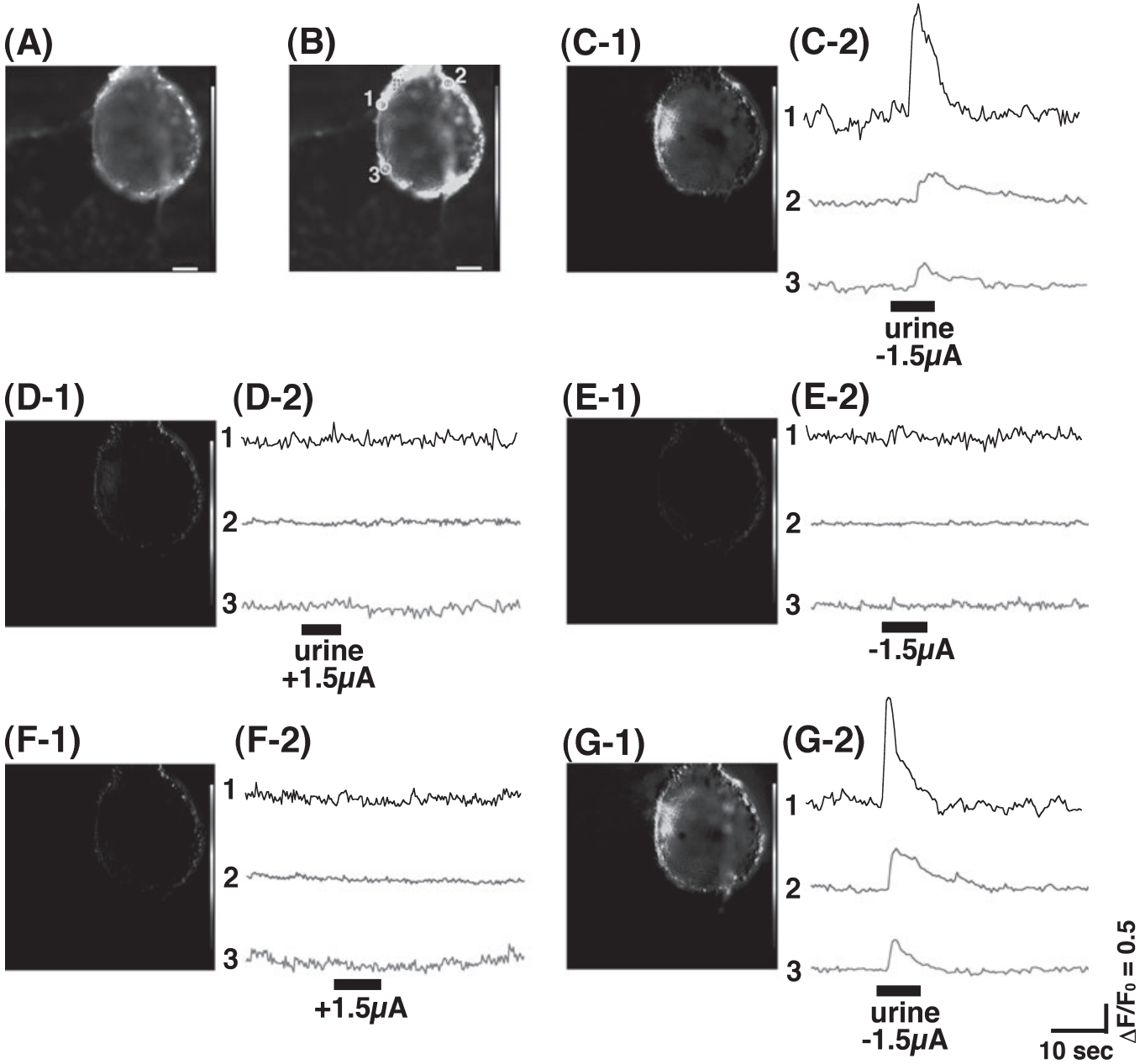

FIG. 5. Specificity and reproducibility of urine-elicited responses in the VNO cocultured with AOB cells. Currents were ejected through a three-barrelled glass microelectrode into the cavity of the VNO at 14 DICC. (A) Fluo-4 fluorescence image of cultured VNO. (B) Fluorescence image showing ROIs, from which changes in fluorescence intensity were recorded. The numbers (1–3) of ROIs correspond to the numbered traces in C-2, D-2, E-2, F-2 and G-2. (C-1–G-1) The subtraction images calculated as $F - F_0$ (F, the average of 25 fluorescence images during current ejection; F_0, the average of 30 fluorescence images just before current ejection). Stimulation protocols were the following: (C-1) urine with a current of −1.5 μA; (D-1) urine with a current of +1.5 μA; (E-1) artificial urine with a current of −1.5 μA; (F-1) artificial urine with a current of +1.5 μA; and (G-1) urine with a current of −1.5 μA again. (C-2–G-2) Time course of changes in fluorescence intensity recorded from the three ROIs shown in B. The application of urine with a current of −1.5 μA (C-2 and G-2) evoked increases in fluorescence intensity, whereas the application of urine with the opposite current or of artificial urine had no effects on fluorescence intensity (D-2, E-2 and F-2).

21 DICC; rat urine: 18.8 ± 2.3%, $n = 7$ at 14 DICC) than in the control groups (2.1 ± 1.0%, $n = 7$, at 14 DICC; 1.4 ± 0.77%, $n = 7$, at 21 DICC; $P < 0.01$ at both DICC, ANOVA followed by Tukey–Kramer multiple comparison test; Fig. 7). The difference between mouse and rat urine at 14 DICC was not statistically significant. Furthermore, the mean relative response areas of the cocultured VNO in the urine groups were significantly larger at 14 DICC than at 7 DICC ($P < 0.01$; Fig. 7). No significant difference between the urine group (2.8 ± 0.77%, $n = 7$) and the control group (2.2 ± 0.57%, $n = 7$) was detected in the VNO-alone culture at 31 DIV (Fig. 7).

Discussion

In the present study, regulation of vomeronasal receptor expression in the VNO was investigated using biochemical, immunocytochemical and functional imaging techniques. We show here that the expression of V2R family vomeronasal receptors in the VNO was enhanced by the presence of its target centre, the AOB, *in vitro*. Immunoblot analyses using specific antibodies to two representatives from the V2R family (VR1 and VR4; Matsunami & Buck, 1997) clearly show that the expression of both receptors in the cultured VNO was enhanced by

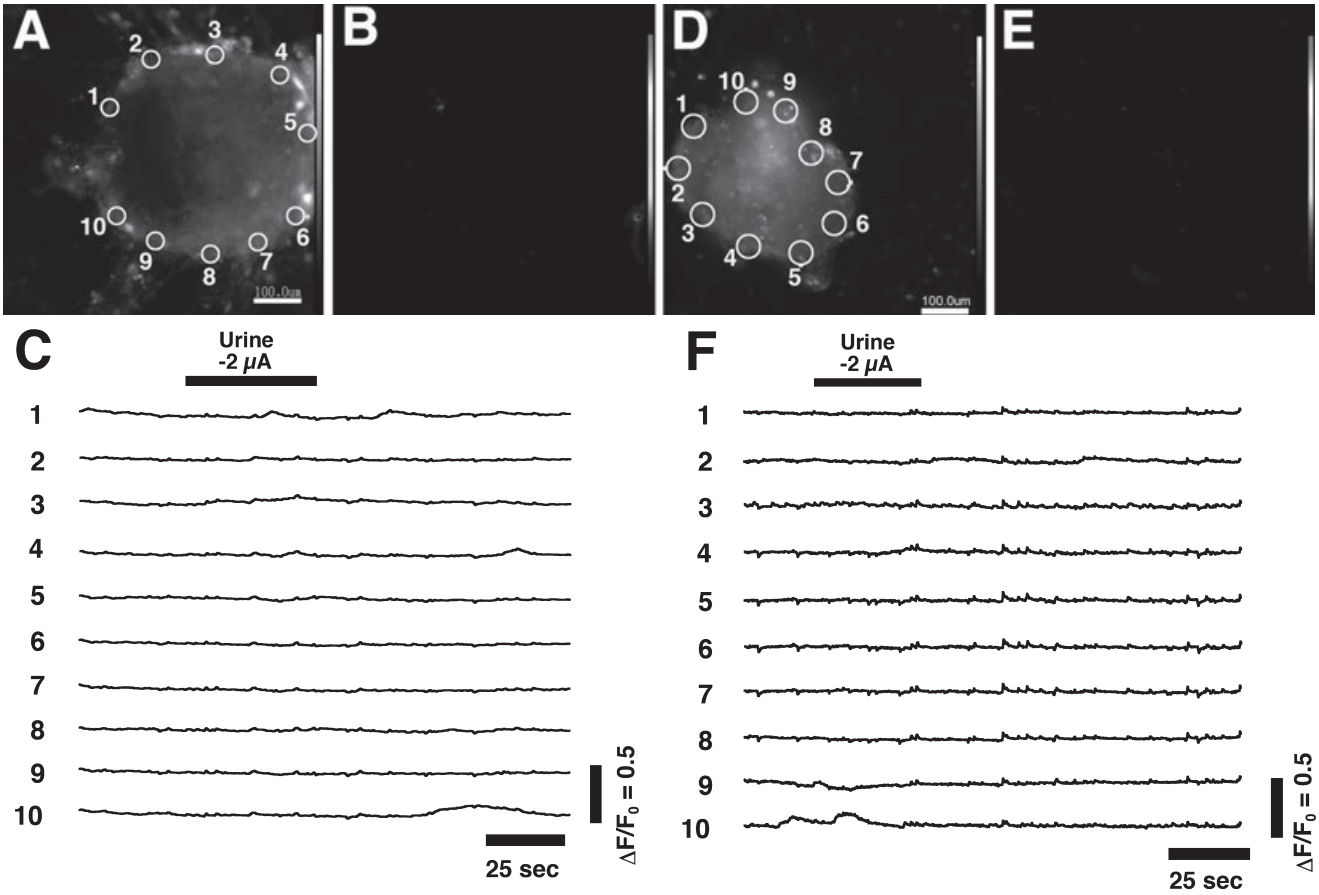

FIG. 6. Responses to urine were not observed in the VNO cultured alone or cocultured with AOB cells at an early time point in coculture. (A–C) Changes in fluorescence intensity of a VNO in the absence of AOB neurons. The VNO, cultured for 10 days, was transferred onto a feeder cell layer and maintained. The changes in the fluorescence intensity were recorded from ROIs shown in (A). The numbers in A correspond to the numbered traces in C. No significant changes in fluorescence intensity were observed during the electrophoretic ejection of charged compounds in the male mouse urine. (B) A subtraction image, which was made by subtracting the image in the resting state (averaging the first 30 images before current ejection) from that in the excitation state (averaging 30 images during current ejection) also indicates that no regions showed significant changes. (D–F) Changes in fluorescence intensity of a VNO at an early time point in coculture. The VNO was maintained for an additional 7 days in coculture with AOB cells and then tested for the response to urine. The numbers in D correspond to the numbered traces in F. No significant changes in fluorescence intensity were observed. A subtraction image (E) was made as described in B.

coculturing with AOB neurons. Furthermore, such enhancement of receptor expression by interacting with the AOB was strongly supported by the functional imaging observation.

Anti-VR1 and -VR4 antibodies used in the present study specifically react with a relevant mouse vomeronasal receptor. Immunoblot analyses using both antibodies showed that a few detectable bands were apparent in whole VNO homogenates from rats as well as mice (Fig. 1). Of these bands, the clearest was observed at $\sim$90 kDa in each lane; this corresponds well with the estimated molecular mass of V2R family vomeronasal receptors. This protein band can equally be observed not in only mouse but also in rat VNO lysate (Fig. 1). Thus, we can consider this band to be a member of the V2R family of vomeronasal receptors. In support of this view, the addition of excess antigenic peptides together with antibodies into the first reaction solution resulted in the disappearance of this band but not other bands (Fig. 1A and B). The densitometric analyses of VR1- and VR4-immunoreactive bands clearly indicate that the expression of immunopositive proteins significantly increased with time in VNO–AOB coculture. Such increases were not observed in the VNO-alone culture, suggesting that the expression of V2Rs in VSNs is enhanced by interacting with the AOB.

Some extra bands were observed in the immunoblot results, in particular in the VR4 immunoblotting (Fig. 1B). Presumably these bands could have been degradation products because most of them showed lower molecular weights than V2Rs, and they disappeared or weakened after the antibodies were absorbed with antigen peptides. These extra bands were not always observed in other experiments.

Immunofluorescent staining clearly showed that the VR4-immunopositive cells were sparsely but certainly distributed throughout cryosections of VNOs cocultured with AOB cells (Fig. 3). These VR4 immunoreactivities were strongly observed around somata and superimposed on tubulin-βIII-immunopositive somata, indicating that VR4-immunopositive cells were neurons, i.e. VSNs. The tubulin-βIII-immunopositive cells in the singly cultured VNOs were decreased in number, conforming to our previous report (Moriya-Ito *et al*., 2005). In addition, we could not observe VR4-immunopositive somata in cryosections of the singly cultured VNOs. These immunofluorescence results strongly support the idea that the VSNs can efficiently mature by interacting with their target, the AOB, and eventually express the subpopulations of vomeronasal receptors.

The microvilli of VSNs in the VNO sensory epithelium project into the VNO lumen and are believed to be the subcellular sites of VSNs that interact with incoming VNO-targeted chemosignals. Most of the VNO signalling molecules, including $G_{i\alpha 2}$, $G_{o\alpha}$ and transient receptor potential channel 2, are localized prominently and selectively in VSN microvilli (Menco *et al*., 2001). Similarly, immunoreactivity for a

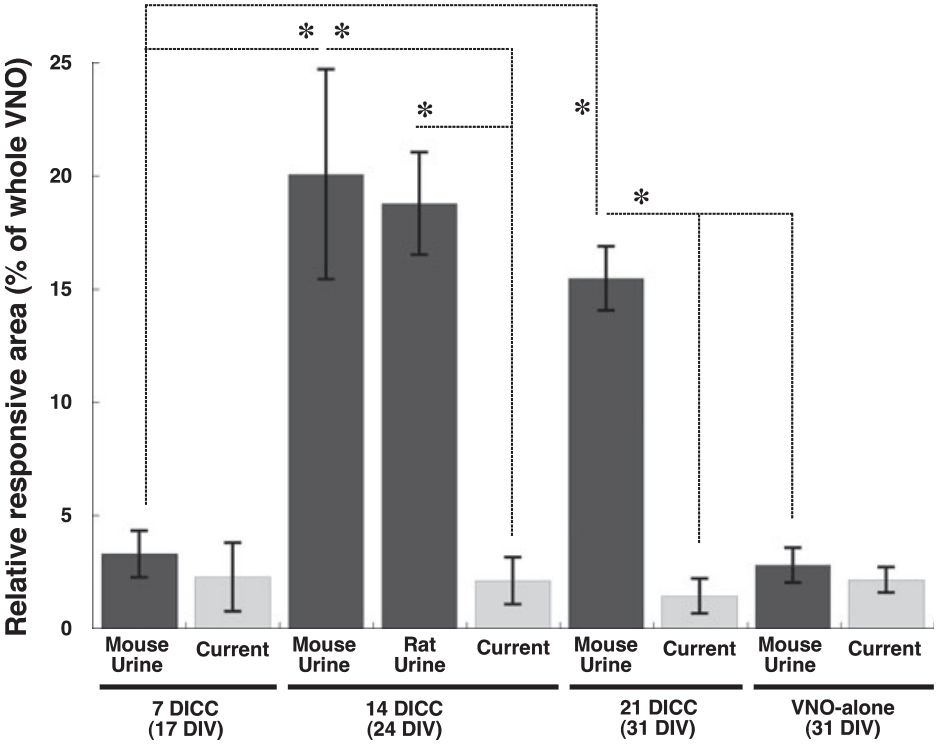

FIG. 7. Bar graph comparing the effects of coculture with AOB cells on urine-elicited response areas of cultured VNOs. A urine-elicited response area was measured using the public software Image-J, and the result expressed as the percentage of response area in the resting whole VNO area. Bars represent means ± SEM ($n = 7$). *$P < 0.01$ (ANOVA followed by Tukey–Kramer multiple comparison test).

vomeronasal receptor is observed on the luminal surface of the VNO sensory epithelium, and is specifically localized at the dendritic knobs and microvilli of VSNs (Takigami *et al*., 1999). Thus, mature VSNs express the vomeronasal receptor densely in the microvilli, which are located near the luminal surface of the sensory epithelium. As previously reported, the maturation of VSNs in culture is induced by coculturing with AOB neurons (Moriya-Ito *et al*., 2005). Cultured VSNs express OMP and develop microvilli which protrude into the central cavity, which is a structural characteristic of cultured VNO (Osada *et al*., 1999) in the presence of AOB neurons (Moriya-Ito *et al*., 2005). This characteristic cavity *in vitro* appears to correspond to the VNO lumen *in vivo* (Osada *et al*., 1999; Moriya-Ito *et al*., 2005). The present immunocytochemical staining showed that the expression of VR4 was localized along the dendritic process and near the surface along the cavity in the cocultured but not in the singly cultured VNO (Fig. 3I and J). Such localization of the vomeronasal receptor may be consistent with that of *in vivo* VSNs. Cultured VSNs express V2R family vomeronasal receptors in the appropriate position by interacting with cocultured AOB neurons.

The next question is whether these inducibly expressed vomeronasal receptors are functional or not. It would have been better if the responses of individual VSNs to urine components could have been recorded. However, we failed to isolate the intracellular Ca^{2+} response of a single VSN from the VNO in organ culture that maintained a spherical structure of 100–200 μm in diameter.

An iontophoretic method enables us to eject only the charged compounds in urine into the cavity of the cultured VNO. In the present study, when only a negative but not a positive current was applied for the ejection of charged compounds in urine, the cocultured VNO showed clear increases in intracellular Ca^{2+}, suggesting that negatively charged materials in urine could evoke a response in cultured VSNs. There are many chemicals in urine, some of which are present in protein or peptide fractions. The VSNs respond to nonvolatile pheromones including peptides (through V2Rs) as well as volatile chemicals (through V1Rs) bound to the MUP family (Krieger *et al*., 1999). MUPs are major components of urinary proteins in rodents and are a highly polymorphic family (Beynon *et al*., 2002), with isoelectric points (pI) in the range pH 4.5–4.9 (Sampsell & Held, 1985). These are thought to have a chemosensory signalling role in a variety of species and behavioural contexts (Flower, 1996).

Alternatively, it has been recognized that behaviours such as mate choice and parent–offspring interactions can be influenced by the MHC genotype (Restrepo *et al*., 2006). Similar to MUPs, MHC molecules are also encoded by a highly polymorphic family of genes that determine immunological identity at the tissue level. Recent evidence has demonstrated that the MHC ligand oligopeptides can function as chemosignals and they are also present in urine (Leinders-Zufall *et al*., 2004; Boehm & Zufall, 2006; Brennan & Zufall, 2006). Each mouse strain expresses a different MHC haplotype, of which MHC class I molecules can bind a variety of peptides that differ in their amino acid sequences but have anchor residues constrained to specific positions along the peptide chain. For example, SYFPEITHI is a prototypical MHC class I ligand peptide for the H-2^d haplotype of BALB/c mice, while AAPDNRETF is for the H-2^b haplotype of C57BL/6 mice (Leinders-Zufall *et al*., 2004). Theoretical pI values of SYFPEITHI and AAPDNRETF are pH 5.22 and 4.37, respectively (calculated using the public domain tool 'ExPASy Compute pI/Mw' at http://au.expasy.org/tools/). Therefore, both MUPs and MHC ligand peptides are negatively charged under the present experimental condition (pH 7.4; see Materials and methods), and appear to be possible candidates for the chemosignals that elicited the VNO response.

When artificial urine and diluted buffer were used instead of natural urine for iontophoretic ejection, no significant changes in intracellular Ca^{2+} were observed. These results indicate that inorganic ions in urine are not effective in eliciting the cultured VNO response. Furthermore, the cultured VNO in the absence of AOB cells did not respond to iontophoretically ejected urine components, suggesting that VSNs cannot acquire enough receptivity for effective compounds in urine until they interact with AOB neurons.

In the present study, responses of cultured VNO were evoked by mouse urine as well as rat urine. Generally, pheromonal signals carry information essential for the reproductive and social behaviour between individuals of the same species (Wysocki & Meredith, 1987). However, it has been reported that the vomeronasal system responds to both conspecific and heterospecific chemosignals at the VNO level, and its central projections site, the vomeronasal amygdala, discriminates between them (Meredith & Westberry, 2004). Both chemosignals induce an immediate behavioural activation, but only species-specific ones lead to a delayed behavioural activation (Mucignat-Caretta *et al*., 2006). In hamsters, the medial amygdala, a projecting site from the AOB, responds categorically differently to conspecific and heterospecific chemosignals, while the VNO and AOB response do not distinguish between con- and hetero- categories (Meredith & Westberry, 2004). Probably, rodents share a similar repertoire of functional vomeronasal receptor genes, as is the case for mice and rats (Dulac & Torello, 2003). It has been proposed that pheromones released from an individual act as a blend of chemicals (Dulac & Torello, 2003). Moreover, con- and heterospecific chemosignals may partially share common chemical components. Common chemicals would activate common vomeronasal receptors but could be components of different blends; each blend might convey the information for only one of the species. The AOB responds in differential spatiotemporal patterns to chemosignals, presumably reflecting stimulation by different chemicals, of VSNs expressing different VRs (Del Punta *et al*., 2002). Different spatiotemporal patterns of AOB response result in categorically different responses to conspecific and heterospecific signals in the amygdala. It has been demonstrated that the anterior medial amygdala in hamsters is equivalently activated by some animal stimuli, including mice and cats, while the posterior medial amygdala shows categorically different responses to conspecific and heterospecific chemosignals (Meredith & Westberry, 2004). Thus, the posterior medial amygdala is considered a central projection area selectively activated by species-specific chemosignals (Mucignat-Caretta *et al*., 2006). Possibly, the spatiotemporal pattern of amygdala input with some criterion is important for eliciting normal species-specific behaviour, and heterospecific stimulation fails to do so because it does not match the required pattern closely enough (Nolte & Meredith, 2005). A similar activation pattern of the anterior and posterior medial amygdala was also reported in rats (Mucignat-Caretta *et al*., 2006), suggesting that the analogous mechanism for discriminating species-specific chemosignals is broadly organized in rodents. Therefore, rat VSNs can detect chemosignals derived from other species including mice.

Although singly cultured VSNs do not show any maturational characteristics (Osada *et al*., 1999; Moriya-Ito *et al*., 2005), they mature following coculture with AOB neurons (Moriya-Ito *et al*., 2005). The enhanced expression of V2Rs involves such *in vitro* maturational processes being affected by coculturing with AOB neurons. It takes 21 DICC to fully detect *in vitro* maturational changes in VSNs (Moriya-Ito *et al*., 2005). More recently we reported that functional synaptic coupling between the cultured VNO and AOB neurons was also detectable at $\sim$21 DICC, in parallel with maturational changes. Such a correlation between the maturation of cultured VSNs and *in vitro* synapse formation suggests that these maturational changes are induced by interaction that occurs via synaptic contact between them (Muramoto *et al*., 2006).

When the VNO is cocultured with AOB neurons but physically separated by an agarose gel divider or is cultured in a conditioned medium collected from the AOB alone culture, the maturational changes disappear in the VNO (Moriya-Ito *et al*., 2005) as well as in the AOB neurons (Ishimatsu *et al*., 2006). These, together with the time-course correlation, suggest that maturational changes in both the VNO and AOB are not induced by soluble trophic factors but by physical contacts between the VSNs and AOB neurons. Although a recent microarray analysis has suggested that fibroblast growth factor signalling controls the expression of vomeronasal receptors during embryogenesis in mice (Lioubinski *et al*., 2006), nonetheless we postulate that the maturation of VSNs is activity-dependently induced by synapse formation between the VSN and AOB neurons.

Generally, electrical activity profoundly affects the development of the nervous system. The means by which this occurs are multiple but include activity-dependent retrograde signals that affect the survival and differentiation of the activity-source neurons (Wingate & Thompson, 1994). It is generally assumed that such effects must involve modulation of the production or release of neurotrophic factors by the postsynaptic cells (Thoenen, 1995). For example, it was reported that the neurotrophin family of proteins retrogradely affected maturation of neurons in the visual system at multiple levels (Wingate & Thompson, 1994; Spalding *et al*., 2002). In the olfactory system, brain-derived neurotrophic factor (BDNF), glial cell line-derived neurotrophic factor (GDNF) and ciliary neurotrophic factor (CNTF) are expressed in the olfactory bulb (Buckland & Cunningham, 1998), although trophic factors in the vomeronasal system have not been clarified yet. Moreover, a few reports indicate that NGF mRNA is highly expressed while NGF receptor mRNA is virtually undetectable in the olfactory bulb, including the AOB, suggesting that the olfactory bulb serves as a target source of NGF for distant afferent neurons (Lu *et al*., 1989). In horses, the NGF receptor TrkA is expressed in the sensory epithelium of the VNO (Garcia-Suarez *et al*., 1997). These trophic factors may be involved in the maturation of the VSN. However, as there is little evidence for the trophic effect in the vomeronasal system, further investigation would be necessary to clarify this issue.

OMP expression in the cultured VNO is induced not only by AOB neurons but also by cells from some nontarget CNS regions, such as the main olfactory bulb and the cerebral cortex (Moriya-Ito *et al*., 2005). By analogy with this evidence, it is assumed that nontarget cells can induce V2R expression as well.

The expression patterns of one V2R receptor vary between males and females in rats, suggesting the existence of discrete and sexually dimorphic patterns of receptor expression (Herrada & Dulac, 1997). A recent report supports this early observation and demonstrates that the expressions of both VR1 and VR4 are sexually dimorphic. The expressions of VR1 and VR4 are differentially modulated by different sex steroid hormones; estradiol suppresses VR1 expression in male mice, while testosterone enhances VR4 expression in males relative to similarly treated females (Alekseyenko *et al*., 2006). Our present results strongly support the idea that the expression of some V2Rs is negatively or positively regulated by various factors, including hormones and the formation of the target connections.

Acknowledgements

This work was supported in part by research grants from the Ministry of Education, Culture, Sports, Science and Technology of Japan and Kochi University to K.M. and H.K. We are grateful to Dr Keiko Moriya-Ito and Hiroko Fujita, Yasuko Hisano and Rie Ito for their technical support.

Abbreviations

AOB, accessory olfactory bulb; BSS, basal salt solution; DICC, days in coculture; DIV, days *in vitro*; MHC, major histocompatibility complex; MUP, major urinary protein; OMP, olfactory marker protein; PBS, phosphate-buffered saline; tubulin-βIII, β-tubulin, class III; VNO, vomeronasal organ; VNP, vomeronasal pocket; VSN, vomeronasal sensory neuron.

References

Alekseyenko, O.V., Baum, M.J. & Cherry, J.A. (2006) Sex and gonadal steroid modulation of pheromone receptor gene expression in the mouse vomeronasal organ. *Neuroscience*, **140**, 1349–1357.

Beynon, R.J., Veggerby, C., Payne, C.E., Robertson, D.H., Gaskell, S.J., Humphries, R.E. & Hurst, J.L. (2002) Polymorphism in major urinary proteins: molecular heterogeneity in a wild mouse population. *J. Chem. Ecol.*, **28**, 1429–1446.

Boehm, T. & Zufall, F. (2006) MHC peptides and the sensory evaluation of genotype. *Trends Neurosci.*, **29**, 100–107.

Brennan, P. & Zufall, F. (2006) Pheromonal communication in vertebrates. *Nature*, **444**, 308–315.

Buckland, M.E. & Cunningham, A.M. (1998) Alterations in the neurotrophic factors BDNF, GDNF and CNTF in the regenerating olfactory system. *Ann. NY Acad. Sci.*, **855**, 260–265.

Del Punta, K., Puche, A., Adams, N.C., Rodriguez, I. & Mombaerts, P. (2002) A divergent pattern of sensory axonal projections is rendered convergent by second-order neurons in the accessory olfactory bulb. *Neuron*, **35**, 1057–1066.

Dulac, C. (2000) Sensory coding of pheromone signals in mammals. *Curr. Opin. Neurobiol.*, **10**, 511–518.

Dulac, C. & Axel, R. (1995) A novel family of genes encoding putative pheromone receptors in mammals. *Cell*, **83**, 195–206.

Dulac, C. & Torello, A.T. (2003) Molecular detection of pheromone signals in mammals: from genes to behavior. *Nat. Rev. Neurosci.*, **4**, 551–562.

Flower, D.R. (1996) The lipocalin protein family: structure and function. *Biochem. J.*, **318**, 1–14.

Garcia-Suarez, O., Germanà, G., Naves, F.J., Ciriaco, E., Represa, J. & Vega, J.A. (1997) Sensory epithelium of the vomeronasal organ express TrkA-like and epidermal growth factor receptor in adulthood. *Anat. Rec.*, **247**, 299–306.

Halpern, M. (1987) The organization and function of the vomeronasal system. *Annu. Rev. Neurosci.*, **10**, 325–362.

Halpern, M. & Martínez-Marcos, A. (2003) Structure and function of the vomeronasal system: an update. *Prog. Neurobiol.*, **70**, 245–318.

Herrada, G. & Dulac, C. (1997) A novel family of putative pheromone receptors in mammals with a topographically organized and sexually dimorphic distribution. *Cell*, **90**, 763–773.

Humphries, R.E., Robertson, D.H.L., Beynon, R.J. & Hurst, J.L. (1999) Unraveling the chemical basis of competitive scent marking in house mice. *Anim. Behav.*, **58**, 1177–1190.

Hurst, J.L., Payne, C.E., Nevison, C.M., Marie, A.D., Humphries, R.E., Robertson, D.H.L., Cavaggioni, A. & Beynon, R.J. (2001) Individual recognition in mice mediated by major urinary proteins. *Nature*, **414**, 631–634.

Ishimatsu, Y., Moriya-Ito, K., Muramoto, K. & Ichikawa, M. (2006) Modification of synapse formation of accessory olfactory bulb neurons by coculture with vomeronasal neurons. *Chem. Senses*, **31**, 371–378.

Kato-Negishi, M., Muramoto, K., Kawahara, M., Hosoda, R., Kuroda, Y. & Ichikawa, M. (2003) Bicuculline induces synapse formation on primary cultured accessory olfactory bulb neurons. *Eur. J. Neurosci.*, **18**, 1343–1352.

Krieger, J., Schmitt, A., Lobel, D., Gudermann, T., Schultz, G., Breer, H. & Boekhoff, I. (1999) Selective activation of G protein subtypes in the vomeronasal organ upon stimulation with urine-derived compounds. *J. Biol. Chem.*, **274**, 4655–4662.

Leinders-Zufall, T., Brennan, P., Widmayer, P., Chandramani, S.P., Maul-Pavicic, A., Jäger, M., Li, X.-H., Breer, H., Zufall, F. & Boehm, T. (2004) MHC class I peptides as chemosensory signals in the vomeronasal organ. *Science*, **306**, 1033–1037.

Leypold, B.G., Yu, C.R., Leinders-Zufall, T., Kim, M.M., Zufall, F. & Axel, R. (2002) Altered sexual and social behaviors in trp2 mutant mice. *Proc. Natl. Acad. Sci. USA*, **99**, 6376–6381.

Lioubinski, O., Alonso, M.T., Alvarez, Y., Vendrell, V., Garrosa, M., Murphy, P. & Schimmang, T. (2006) FGF signalling controls expression of vomeronasal receptors during embryogenesis. *Mech. Dev.*, **123**, 17–23.

Lu, B., Buck, C.R., Dreyfus, C.F. & Black, I.B. (1989) Expression of NGF and NGF receptor mRNA in the developing brain: evidence for local delivery and action of NGF. *Exp. Neurol.*, **104**, 191–199.

Manders, M.M., Verbeek, F.J. & Aten, J.A. (1983) Measurement of co-localization of objects in dual-color confocal images. *J. Microsc.*, **169**, 375–382.

Matsunami, H. & Buck, L.B. (1997) A multigene family encoding a diverse array of putative pheromone receptors in mammals. *Cell*, **90**, 775–784.

Menco, B.P.M., Carr, V.M., Ezeh, P.I., Liman, E.R. & Yankova. M.P. (2001) Ultrastructural localization of G-proteins and the channel protein TRP2 to microvilli of rat vomeronasal receptor cells. *J. Comp. Neurol.*, **438**, 468–489.

Meredith, P. (1991) Sensory processing in the main and accessory olfactory system: comparisons and contrasts. *J. Steroid Biochem. Mol. Biol.*, **39**, 601–614.

Meredith, P. & Westberry, J.M. (2004) Distinctive responses in the medial amygdala to same-species and different-species pheromones. *J. Neurosci.*, **24**, 5719–5725.

Mombaerts, P. (2004) Genes and ligands for odorant, vomeronasal and taste receptors. *Nat. Rev. Neurosci.*, **5**, 263–278.

Moriya-Ito, K., Osada, T., Ishimatsu, Y., Muramoto, K., Kobayashi, T. & Ichikawa, M. (2005) Maturation of vomeronasal receptor neurons in vitro by coculture with accessory olfactory bulb neurons. *Chem. Senses*, **30**, 111–119.

Mucignat-Caretta, C., Colivicchi, M.A., Fattori, M., Ballini, C., Bianchi, L., Gabai, G., Cavaggioni, A. & Corte, L.D. (2006) Species-specific chemosignals evoke delayed excitation of the vomeronasal amygdala in freely-moving female rats. *J. Neurochem.*, **99**, 881–891.

Muramoto, K., Huang, G.-Z., Taniguchi, M. & Kaba, H. (2006) Functional synapse formation between cultured rat accessory olfactory bulb neurons and vomeronasal pockets. *Neuroscience*, **141**, 475–486.

Muramoto, K., Kato-Negishi, M., Kuroda, Y., Kaba, H. & Ichikawa, M. (2004) Differences in development and cellular composition between neuronal cultures of rat accessory and main olfactory bulbs. *Anat. Embryol.*, **209**, 129?136.

Muramoto, K., Osada, T., Kato-Negishi, M., Kuroda, Y. & Ichikawa, M. (2003) Increase in the number of tyrosine hydroxylase-containing neurons in a primary culture system of the rat accessory olfactory bulb by co-culture with vomeronasal pockets. *Neuroscience*, **116**, 985–994.

Nolte, C.M. & Meredith, M. (2005) mGluR2 activation of medial amygdala input impairs vomeronasal organ-mediated behavior. *Physiol. Behav.*, **86**, 314–323.

Osada, T., Ikai, A., Costanzo, R.M., Matsuoka, M. & Ichikawa, M. (1999) Continual neurogenesis of vomeronasal neurons in vitro. *J. Neurobiol.*, **40**, 226–233.

Restrepo, D., Lin, W., Salcedo, E., Yamazaki, K. & Beauchamp, G. (2006) Odortypes and MHC peptides: complementary chemosignals of MHC haplotype? *Trends Neurosci.*, **29**, 604–609.

Sampsell, B.M. & Held, W.A. (1985) Variation in the major urinary protein multigene family in wild-derived mice. *Genetics*, **109**, 549–568.

Spalding, K.L., Tan, M.M.L., Hendry, I.A. & Harvey, A.R. (2002) Anterograde transport and trophic actions of BDNF and NT-4/5 in the developing rat visual system. *Mol. Cel. Neurosci.*, **19**, 485–500.

Takigami, S., Osada, T., Yoshida-Matsuoka, J., Matsuoka, M., Mori, Y. & Ichikawa, M. (1999) The expressed localization of rat putative pheromone receptors. *Neurosci. Lett.*, **272**, 115–118.

Thoenen, H. (1995) Neurotrophins and neuronal plasticity. *Science*, **270**, 593–598.

Wingate, R.J.T. & Thompson, I.D. (1994) Targeting and activity-related dendritic,pdofocatopm om mammalian retinal ganglion cells. *J. Neurosci.*, **14**, 6621–6637.

Wyatt, T.D. (2003) *Pheromones and Animal Behaviour.* Cambridge University Press, Cambridge, UK.

Wysocki, C.J. (1979) Neurobehavioral evidence for the involvement of the vomeronasal system in mammalian reproduction. *Neurosci. Biobehav. Rev.*, **3**, 301–341.

Wysocki, C. & Meredith, M. (1987) The vomeronasal system. In Finger, T.H. & Silver, W.L. (eds), *Neurobiology of Taste and Smell*. Wiley, New York, pp. 125–150.